Computer-Aided Design 58 (2015) 189–199

Contents lists available at ScienceDirect

Computer-Aided Design

journal homepage: www.elsevier.com/locate/cad

ℓ_1-Regression based subdivision schemes for noisy data☆

Ghulam Mustafa [a,b], Hao Li [a], Juyong Zhang [a,*], Jiansong Deng [a]

[a] School of Mathematical Sciences, University of Science and Technology of China, China
[b] Department of Mathematics, The Islamia University of Bahawalpur, Pakistan

HIGHLIGHTS

- An ℓ_1-regression based subdivision scheme is proposed to handle noisy curve/surface data with outliers.
- A fast numerical optimization method named dynamic iterative reweighted least squares is proposed to solve this problem.
- The most advantage of the proposed method is that it removes noises and outliers without any prior information about the input data.

ARTICLE INFO

Keywords:
ℓ_1-Regression
Data restoration
Outlier detection
Subdivision scheme
Iterative reweighted least squares

ABSTRACT

Fitting curve and surface by least-regression is quite common in many scientific fields. It, however cannot properly handle noisy data with impulsive noises and outliers. In this article, we study ℓ_1-regression and its associated reweighted least squares for data restoration. Unlike most existing work, we propose the ℓ_1-regression based subdivision schemes to handle this problem. In addition, we propose fast numerical optimization method: dynamic iterative reweighted least squares to solve this problem, which has closed form solution for each iteration. The most advantage of the proposed method is that it removes noises and outliers without any prior information about the input data. It also extends the least square regression based subdivision schemes from the fitting of a curve to the set of observations in 2-dimensional space to a p-dimensional hyperplane to a set of point observations in $(p+1)$-dimensional space. Wide-ranging experiments have been carried out to check the usability and practicality of this new framework.

© 2014 Elsevier Ltd. All rights reserved.

1. Introduction and related work

The curve and surface fitting is the process of constructing curve and surface that has the best fit to the data. In statistics and machine learning, overfitting occurs when a statistical model describes random error or noise instead of the underlying relationship. Overfitting generally occurs when a model is excessively complex. Situation becomes more worse when some data points deviate so much from the other data points as to arouse suspicions in data. Such type of data points are called outliers. Outliers are also referred to as abnormalities, discordants, deviants, or anomalies in the data mining and statistics literature. Outlier detection and dealing with noisy data have been extensively studied in the past decades in different disciplines. Here is the brief survey of the related work.

One of the most widely used statistical technique to detect outlier is weighted least squares regression [1]. In 1997, Sohn and Kim [2] proposed an algorithm for detection of outliers in weighted least squares regression using Studentized weighted residuals. Multiple case outlier detection in least squares regression model using quantum inspired evolutionary algorithm has been introduced by Khan and Aktar [3]. Iteratively reweighted minimization algorithms for sparse recovery and matrix rank minimization have been discussed by [4–6]. Bissantz et al. [7] offered convergence analysis of generalized iteratively reweighted least squares algorithms on convex function spaces by using quantile, ℓ_q, $q \in [1, 2)$ logistic and isotonic regressions. Lai et al. [8] presented improved iteratively reweighted least squares for unconstrained smoothed ℓ_q, $q \in (0, 1]$ minimization. However, the detection of outlier in high dimensional case is a challenging task. This is because in high dimensionality, the data becomes sparse and the sparsity behavior makes all points look very similar and almost equidistance to one another. A practical algorithm to outlier detection and data cleaning for the time-dependent signal is proposed by Pan et al. [9]. It is claimed that proposed algorithm is good for bioinformatic application. Nikolova [10] introduced ℓ_1 data-fidelity based variational

☆ This paper has been recommended for acceptance by Dr. Vadim Shapiro.

* Corresponding author. Tel.: +86 551 63600673.
E-mail addresses: ghulam.mustafa@iub.edu.pk (G. Mustafa), lihao215@mail.ustc.edu.cn (H. Li), juyong@ustc.edu.cn (J. Zhang), dengjs@ustc.edu.cn (J. Deng).

http://dx.doi.org/10.1016/j.cad.2014.08.003
0010-4485/© 2014 Elsevier Ltd. All rights reserved.

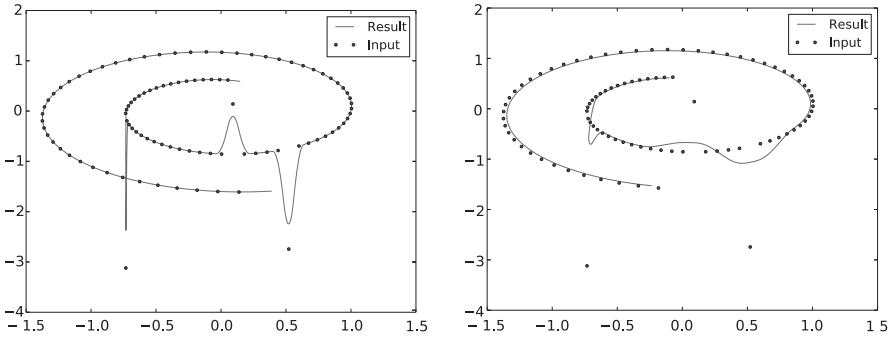

(a) Classical scheme. (b) *LS* scheme.

Fig. 1. Points are fitted by classical Chaikin scheme (i.e. quadratic B-spline) [29] and least square regression based subdivision scheme. Solid filled circles are initial data with outliers.

method for the processing of image corrupted with outliers and different kinds of impulse noise. Avron et al. [11] introduced an ℓ_1-sparse method for the reconstruction of a piecewise smooth point set surface. Optimal fitting may alternatively be obtained using simpler functions and the ℓ_1 and ℓ_∞ norms [12].

The class of ℓ_1-regularized optimization problems has received much attention recently because of the introduction of compressed sensing [13], which allows images and signals to be reconstructed from small amounts of data. Despite this recent attention, many ℓ_1-regularized problems still remain difficult to solve, or require techniques that are very problem-specific [14]. Yang and Zhang [15] studied the use of alternating direction algorithms for several ℓ_1-norm minimization problems arising from sparse solution recovery in compressive sensing. A new nonlocal total variation regularization algorithm for image denoising has been introduced by Liu and Huang [16]. Xiao et al. [17] proposed, analyzed and tested primal and dual versions of the alternating direction algorithm for the sparse signal reconstruction from its major noise contained observation data. The algorithm minimizes a convex non-smooth function consisting of the sum of ℓ_1-norm regularization term and ℓ_1-norm data fidelity term. Candès et al. [18] presented a novel method for sparse signal recovery that in many situations outperforms ℓ_1-minimization in the sense that substantially fewer measurements are needed for exact recovery. The algorithm consists of solving a sequence of weighted ℓ_1-minimization problems where the weights used for the next iteration are computed from the value of the current solution.

Subdivision schemes (i.e. classical schemes) are widely used for curve and surface fitting from few decades. An intensive study and literature along with mathematical descriptions and formulations are available now [19–23]. A major advantage of subdivision schemes is that they can be easily applied to virtually any data type. However, early work in subdivision schemes does not deal with noisy data with impulsive noises and outliers. A downside of subdivision algorithm is that they are sensitive to outliers. One outlier can damage whole model and in most of the cases, schemes give overfitted model for noisy data with outliers. One algorithm has been reported by [24] for fitting a Catmull–Clark subdivision surface model to an unstructured, incomplete and noisy stereo data set by using quasi-interpolation technique but this work does not deal with outliers. Recently, Dyn et al. [25] have presented univariate subdivision schemes based on least squares minimization to deal with noisy data. They have compared their schemes with least squares minimization problems with kernel weights. The main purpose of their work was to address an open question: How to approximate a function from its normally distributed noisy samples by subdivision schemes?

The purpose of our article is to address the open question: How can we approximate a function by subdivision technique from its noisy samples with impulsive noises and outliers? To address this question: we use the ℓ_1-regression to construct subdivision schemes with dynamic iterative reweighted weights. Numerical results show that new schemes have the ability to remove outliers and give better fitted models as compared to the other subdivision schemes when data is contaminated with noises and outliers. A major advantage of our schemes is that they give best fit to any type of data with and without added noise and outliers in high dimensional spaces. Throughout this paper, *LS* scheme means subdivision scheme based on least square regression with constant weights while ℓ_1 scheme means subdivision scheme based on ℓ_1-regression with dynamic iterative reweighted weights.

The paper is structured as follows: In Section 2, the construction of ℓ_1 scheme for curve fitting is discussed in detail along with its variants. Numerical examples for curve fitting are also presented in this section. In Section 3, we introduce ℓ_1 scheme for surface fitting. We also introduce new least square regression surface schemes in this section as special cases of ℓ_1 schemes. Comparison of fitting surfaces by ℓ_1 and *LS* schemes is also presented in this section. Section 4 summarizes the topics discussed in this article and outlines further research directions.

2. ℓ_1 scheme for curve fitting

In this section, we propose a class of ℓ_1-regression based subdivision schemes with dynamic iterative reweighted weights for curve fitting. We also discuss its generalization and variants along with some numerical experiments.

2.1. Motivation

There exists vast classical subdivision-based literature of fitting curves and surfaces to a given data set in Geometric Modeling. But this literature does not deal with noisy data along with outliers (see Fig. 1(a)). Although a class of least square regression based subdivision schemes [25] are good to deal with normally distributed noisy data but these do not seem reasonable to deal with outliers. Fig. 1(b) shows a fitted curve to a data with outliers by least square regression based subdivision scheme. A significant perturbation has been occurred in the fitted curve due to outliers. This is because the outlier has big distance value to the fitting curve, however, in ℓ_1-regression, it is not penalized too much, while in least square regression based model, the distance is squared, and thus it has a big impact to the objective energy. Also ℓ_1-regression based procedure is more robust to the presence of outlying observations [26]. So we propose to initiate a new class of subdivision schemes based on ℓ_1-regression for fitting noisy data with impulsive noises and outliers.

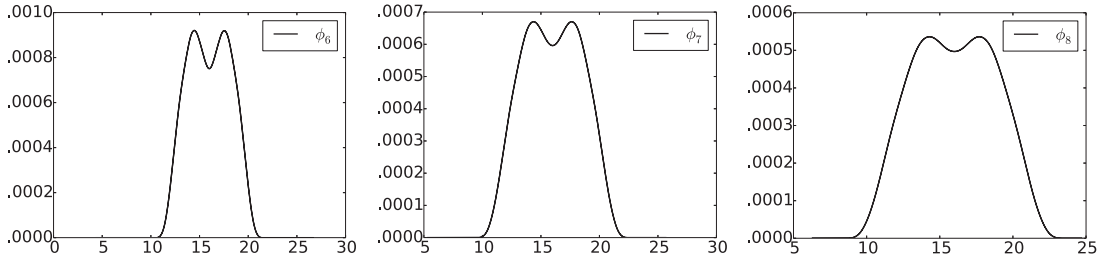

Fig. 2. Basic limit functions ϕ_6, ϕ_7, ϕ_8, of ℓ_1 schemes D_6, D_7, D_8..

2.2. Our approach

The straight-line regression based on weighted least squares is a procedure to determine the best line fit to data. The basic problem is to find the best fit straight line $f(x) = \beta_1 + \beta_2 x$ with respect to the observations $(x_r = r, f_r)$ for $r = -n+1, \ldots n$, where $n > 0$. In robust statistics [27], ℓ_1 fitting function was found useful to make estimation reliable. The ℓ_1-norm operator can be expressed as

$$\min_{\beta_1,\beta_2\in\mathbb{R}} \sum_{r=-n+1}^{n} |f_r - (\beta_1 + \beta_2 r)|$$

which is also called ℓ_1-regression problem. In order to estimate β_1 and β_2, without loss of generality, we express the optimization of β_1 and β_2 as

$$\begin{aligned}\beta_1, \beta_2 &= \arg\min_{\beta_1,\beta_2\in\mathbb{R}} \sum_{r=-n+1}^{n} |f_r - \beta_1 - \beta_2 r| \\ &= \arg\min_{\beta_1,\beta_2\in\mathbb{R}} F(\beta_1, \beta_2). \end{aligned} \tag{1}$$

It cannot be solved the same way as least square regression owing to the lack of differentiability. We resort to the iterative reweighted least squares (IRLS) [7]. The IRLS is based on the idea that, in a first step, the ℓ_1 norm F, being a convex functional, can be regularized/approximated by a family of smooth convex functionals F_δ, $\delta > 0$, i.e.

$$F_\delta(\beta_1, \beta_2) = \sum_{r=-n+1}^{n} h_\delta\left(f_r - \beta_1 - \beta_2 r\right), \quad \text{where}$$

$$h_\delta\left(f_r - \beta_1 - \beta_2 r\right) = \left[(f_r - \beta_1 - \beta_2 r)^2 + \delta\right]^{1/2}. \tag{2}$$

The regularization of a non-smooth functional as in (1) by (2) is well known by [28]. Since $\beta_{1,\delta}, \beta_{2,\delta} = \arg\min_{\beta_1,\beta_2\in\mathbb{R}} F_\delta(\beta_1, \beta_2)$ is approximation of β_1, β_2 by ([7], Theorem 1). So in order to compute $\beta_{1,\delta}, \beta_{2,\delta}$ the following iterative formula for $m \geqslant 0$ and $n \geqslant 1$, can be used

$$\beta_{1,\delta}^{(m+1)}, \beta_{2,\delta}^{(m+1)} = \arg\min_{\beta_1,\beta_2\in\mathbb{R}} \sum_{r=-n+1}^{n} w_r^{(m)} (f_r - \beta_1 - r\beta_2)^2, \tag{3}$$

where $w_r^{(m)} = 1/\left[(f_r - \beta_{1,\delta}^{(m)} - r\beta_{2,\delta}^{(m)})^2 + \delta\right]^{1/2}$. As a starting value $\beta_{1,\delta}^{(0)}, \beta_{2,\delta}^{(0)}$ any simple least squares estimator can be used. Each iteration of above formula involves minimizing a quadratic objective function. Iterations are continued until

$$\max\left(\left|\beta_{1,\delta}^{(m+1)} - \beta_{1,\delta}^{(m)}\right|, \left|\beta_{2,\delta}^{(m+1)} - \beta_{2,\delta}^{(m)}\right|\right) < \epsilon.$$

The global optimum can be reached by taking derivatives of (3) and setting them to zero. This leads to the following solution of system of linear equations.

$$\beta_{2,\delta}^{(m+1)} = \sum_{r=-n+1}^{n} \frac{r\tau_1^{(m)} - \tau_2^{(m)}}{\tau_1^{(m)}\tau_3^{(m)} - \left(\tau_2^{(m)}\right)^2} w_r^{(m)} f_r,$$

$$\beta_{1,\delta}^{(m+1)} = \frac{1}{\tau_1^{(m)}} \sum_{r=-n+1}^{n} w_r^{(m)} f_r - \beta_{2,\delta}^{(m+1)} \left(\frac{\tau_2^{(m)}}{\tau_1^{(m)}}\right),$$

where

$$\tau_1^{(m)} = \sum_{r=-n+1}^{n} w_r^{(m)},$$

$$\tau_2^{(m)} = \sum_{r=-n+1}^{n} r w_r^{(m)},$$

$$\tau_3^{(m)} = \sum_{r=-n+1}^{n} (r)^2 w_r^{(m)}.$$

By substituting optimum $\beta_{1,\delta}^{(m+1)}$, $\beta_{2,\delta}^{(m+1)}$ of β_1, β_2 into the linear function $f(x) = \beta_1 + \beta_2 x$ and evaluating this function at $1/4$ and $3/4$ then changing notations, we get closed form of ℓ_1 scheme for the fitting of noisy data with impulsive noises and outliers shown in Appendix A.

2.3. Overview of ℓ_1 scheme

The ℓ_1 scheme D_{2n} has two main iterative steps. In first step, it assigns the dynamic weights to only $2n$ local initial points then these weights are iteratively reweighted. During this process the outliers (if any) among these local $2n$ points have been killed (or assigned less weight). Also noisy sample points assign less weights during this step.

Second step comprises two rules: the topological rule and subdivision rule. The topological rule describes how the refined mesh is created from the original mesh. The subdivision rule computes the locations of the vertices of the new mesh by taking a linear combination of the local $2n$ points with iterative dynamic weights assigned by step one to these points. These steps are carried out for next local $2n$ points. In other words subdivision rule computes the locations of the vertices of the new mesh and topological rule describes how many new vertices are added to the mesh and which vertices in the new mesh are connected by edges.

Both iterative steps are repeated for next level of iteration. These steps continue until the resulting curve / polygon become sufficiently smooth. If all the dynamic weight $w_r^{(m)} = 1$ then iterative ℓ_1-regression problem (3) switch over to *LS*-regression. As a result ℓ_1 scheme turns into *LS* scheme. The subscript $2n$ of the ℓ_1 scheme D_{2n} is called complexity of the scheme. We suggest $n \geqslant 3$ for better results.

2.4. Basic limit functions

If $\Delta = \{(-m, 0), \ldots, (-2, 0), (-1, 0), (0, 1), (1, 0), (2, 0), \ldots, (m, 0)\}$, for sufficiently large integer m then the basic limit functions of the schemes D_{2n} and D_{2n+1} are defined as $\phi_{2n} = D_{2n}^{\infty}\Delta$ and $\phi_{2n+1} = D_{2n+1}^{\infty}\Delta$. The basic limit functions ϕ_6, ϕ_7, ϕ_8, of the schemes D_6, D_7, D_8 are shown in Fig. 2. From this figure we see that the effect of these schemes away from the sample $(0, 1)$ is zero so

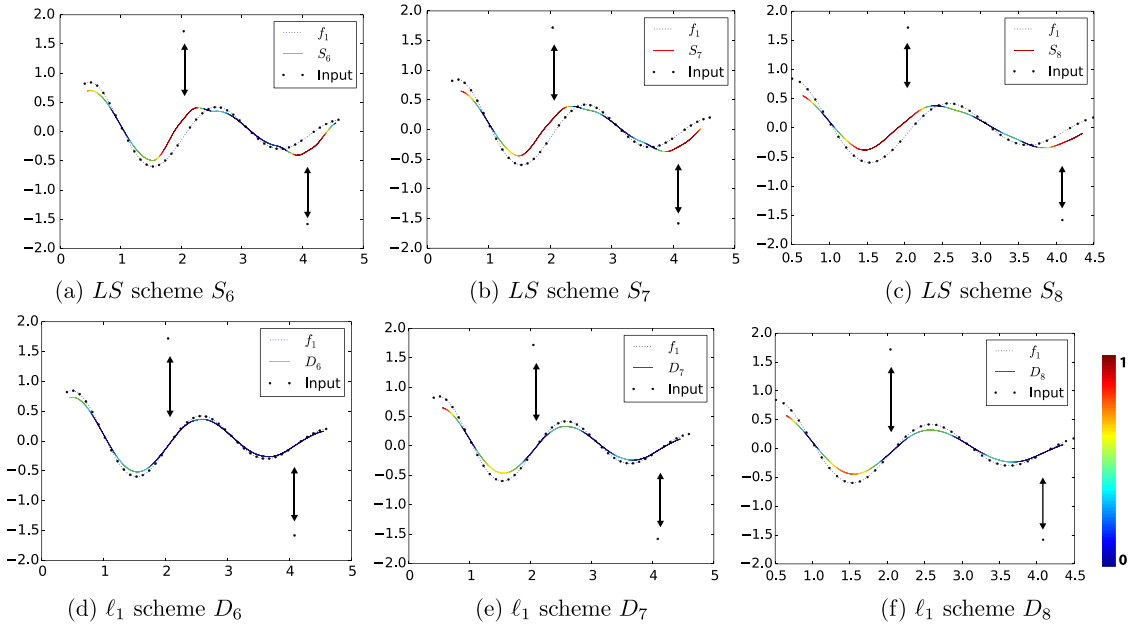

Fig. 3. Effect of outliers: Two outliers are presented in the initial data. Arrows indicate outliers and their effect on fitting curve. The color of each point represents the reconstruction error, and the errors are normalized to [0, 1]. (For interpretation of the references to colour in this figure legend, the reader is referred to the web version of this article.)

these schemes are locally supported. It is also observed that basic limit functions of D_6, D_7, D_8 are smooth enough and have two top peaks with one steep valley.

The support of basic limit functions and subdivision scheme is the area of the limit curve that will be affected by the displacement of a single control point. That part which is dependent on a given control point is called the support width / region of that point. The following proposition is related to the support of basic limit function of the scheme D_{2n}.

Proposition 1. *The basic limit function defined by the scheme D_{2n} has support width $4n-1$, which implies that it vanishes outside the interval $\left[-\frac{4n-1}{2}, \frac{4n-1}{2}\right]$.*

Proof. Since the basic limit function is the limit function of the scheme D_{2n}, its support width can be determined by computing how far the effect of the nonzero vertex $f_0^{(0)}$ will propagate along by. As the mask of the scheme is a $4n$-long sequence by centering it on that vertex, the distances to the last of its left and right nonzero coefficients are equal to $2n$ and $2n-1$ respectively. At the first subdivision step we see that the vertices on the left and right sides of $f_0^{(1)}$ at $\frac{2n}{2}$ and $\frac{2n-1}{2}$ are the furthest nonzero new vertices. At each refinement, the distance on both sides is reduced by the factor $\frac{1}{2}$. At the next step of the scheme this will propagate along by $\frac{2n}{2^2}$ on left and $\frac{2n-1}{2^2}$ on right. Hence after k subdivision steps the furthest nonzero vertex on the left will be at

$$2n\left(\frac{1}{2}+\frac{1}{2^2}+\frac{1}{2^3}+\cdots+\frac{1}{2^k}\right)=\frac{2n}{2}\left(\sum_{j=0}^{k-1}\frac{1}{2^j}\right)$$

and

$$(2n-1)\left(\frac{1}{2}+\frac{1}{2^2}+\frac{1}{2^3}+\cdots+\frac{1}{2^k}\right)=\frac{(2n-1)}{2}\left(\sum_{j=0}^{k-1}\frac{1}{2^j}\right).$$

Since $\frac{1}{2} < 1$, the geometric sequence can be summed to give the extended distance on each side and we conclude that, in the limit, the total influence of the original nonzero vertex will propagate along by

$$\frac{2n}{2}\left(\sum_{j=0}^{k-1}\frac{1}{2^j}\right)+\frac{2n-1}{2}\left(\sum_{j=0}^{k-1}\frac{1}{2^j}\right)=4n-1.$$

This completes the proof. □

2.5. Numerical experiments

In this section, we present intrinsic comparisons among ℓ_1 schemes and corresponding *LS* schemes. We present several experiments to illustrate the performances of fitting curves generated by these schemes from input noisy data with outliers or impulsive. The fitting performance is also characterized by the fitting error. The fitting error for each point is displayed through the jet colorbar as shown in Fig. 3, where the fitting errors are normalized to [0, 1]. All sub-figures use the same normalization (color code).

Experiment 1: In our first experiment, we apply ℓ_1 and *LS* schemes to fit data sample from function $\mathbf{f}_1(x) = \sin(3x)e^{-\frac{x}{3}}$ with two outliers to see the effect of these outliers on fitting curves. It is observed from Fig. 3 that fitting curves generated by S_6, S_7, S_8 are greatly effected by outliers. But D_6, D_7, D_8 do not give response to these outliers. Arrows in this figure indicate outliers and their effect on fitting curves. Since an outlier sample assign a small corresponding weight defined in (6) then in turn enhancing outlier rejection (or a small response) by scheme (4). Large complexity schemes also give less response to outliers than small complexity schemes. This is one of the reasons that small complexity schemes are more effected by outliers than other schemes. If $f_i^{(k)} = (f_{x_i}^{(k)}, f_{y_i}^{(k)})$ then the fitting performance is characterized by the error i.e. the average of the square of the fitting value $f_{y_i}^{(k)}$ and real value $\mathbf{f}_1(f_{x_i}^{(k)})$

$$\text{Error} = \frac{\sum_i \left[f_{y_i}^{(k)} - \mathbf{f}_1(f_{x_i}^{(k)})\right]^2}{N},$$

where N is the total number of fitting values. The fitting errors are summarized in Table 1.

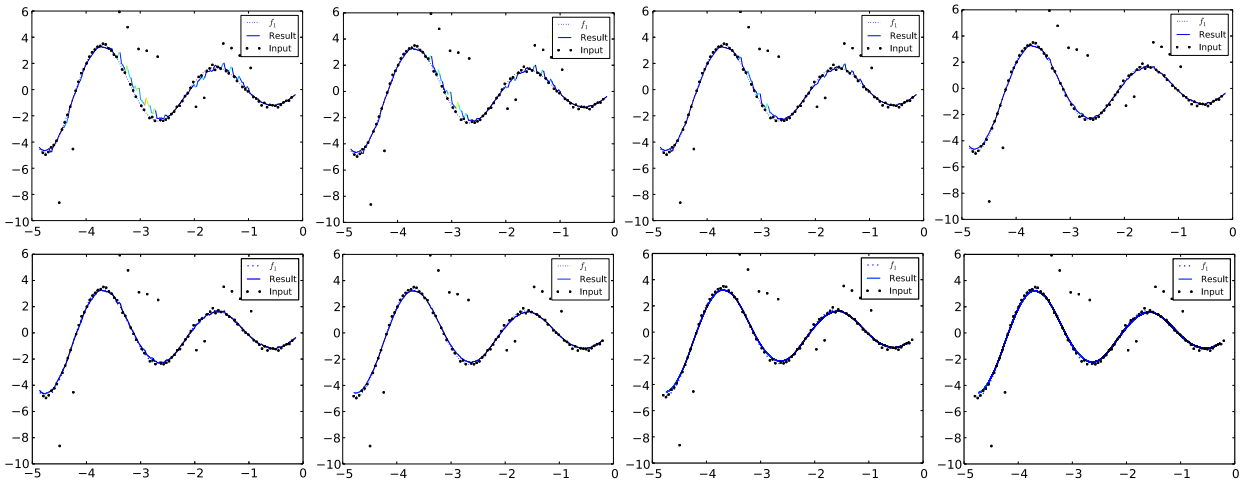

Fig. 4. The first row shows the middle results after iteration 1, 2, 4, 10 in the first subdivision step; The second row shows the results after 1, 2, 4, 6 times subdivision.

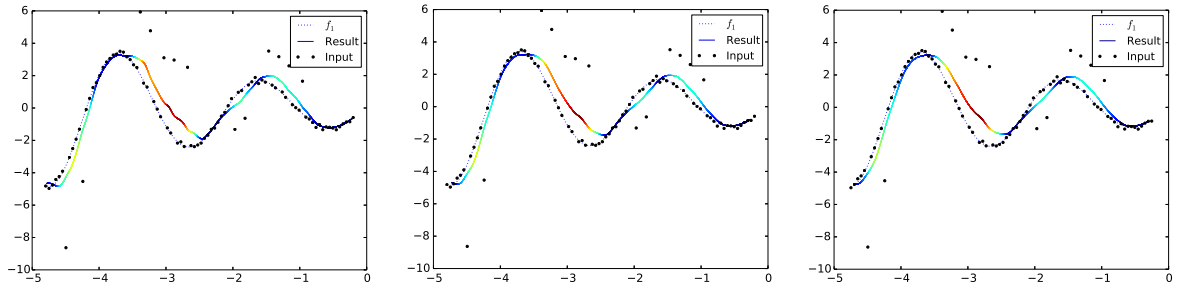

(a) *LS* scheme S_6. (b) *LS* scheme S_7. (c) *LS* scheme S_8.

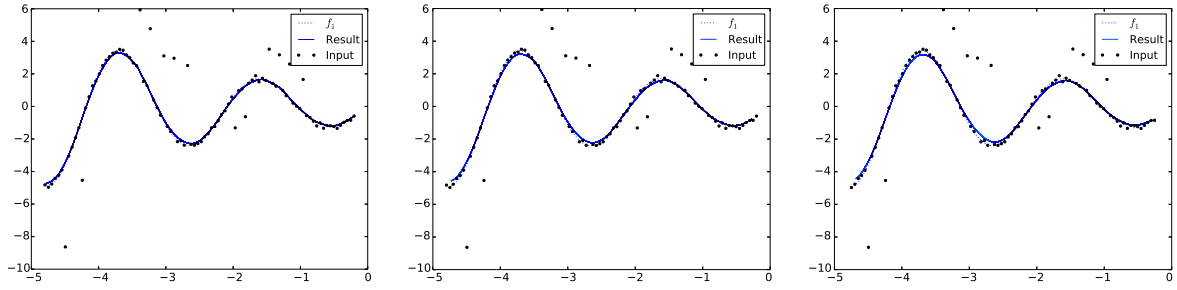

(d) ℓ_1 scheme D_6. (e) ℓ_1 scheme D_7. (f) ℓ_1 scheme D_8.

Fig. 5. Effect of noise and outliers: Thirteen outliers are presented in an initial data. Solid curves are generated by ℓ_1 and *LS* schemes while dash curves are original curve. Filled solid circles are noisy data with outlier.

Table 1
Comparison: Error between fitting curves shown in Fig. 3 and original function $\mathbf{f}_1$.

LS schemes	S_6	S_7	S_8
Errors	0.325824	0.300979	0.300560
ℓ_1 schemes	D_6	D_7	D_8
Errors	0.115044	0.179849	0.175459

Table 2
Comparison: Error between fitting curves shown in Fig. 5 and original function $\mathbf{f}_1$.

LS schemes	S_6	S_7	S_8
Errors	1.485318	1.498197	1.511984
ℓ_1 schemes	D_6	D_7	D_8
Errors	0.197140	0.281907	0.315305

Experiment 2: In second experiment, we generate data from the same function $\mathbf{f}_1(x)$ with Gaussian noise of mean zero and variance 0.1 along with thirteen outliers. Our findings in Experiment 1 are also supported by Experiment 2. Fitting curves by ℓ_1 and *LS* schemes are shown in Fig. 5. Fitting errors between fitting curve and original function are shown in Table 2. We observe that overall ℓ_1 schemes have better performance than *LS* schemes in terms of visual fitting and error between fitting curve and original function when data is noisy along with outliers. We also notice that low complexity schemes give more response to outlier, and to noise so these schemes have more error. Since high complexity schemes give less response to outliers, noise and even to real sample values so these schemes also have more error than low complexity schemes. The scheme D_6 offers better fitted results than other schemes. Our claim is supported by this experiment as well as by other experiments.

The iterative results of our proposed scheme are shown in Fig. 4 for this example (Fig. 5). We can see that the fitting curve gets further improved as iterations increase.

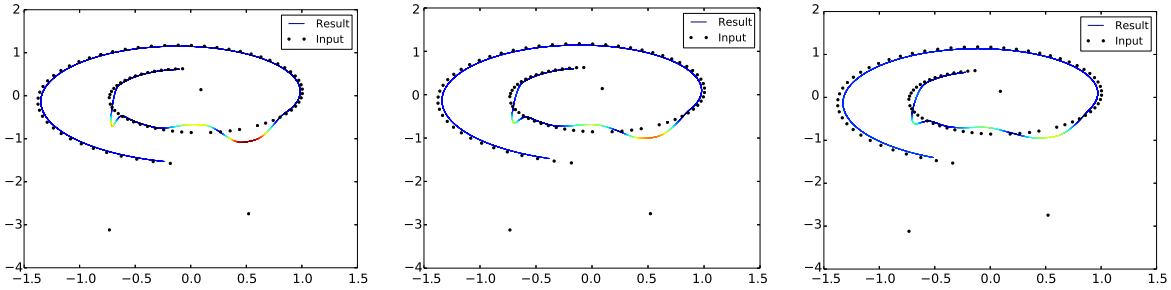

(a) *LS* scheme S_6. (b) *LS* scheme S_7. (c) *LS* scheme S_8.

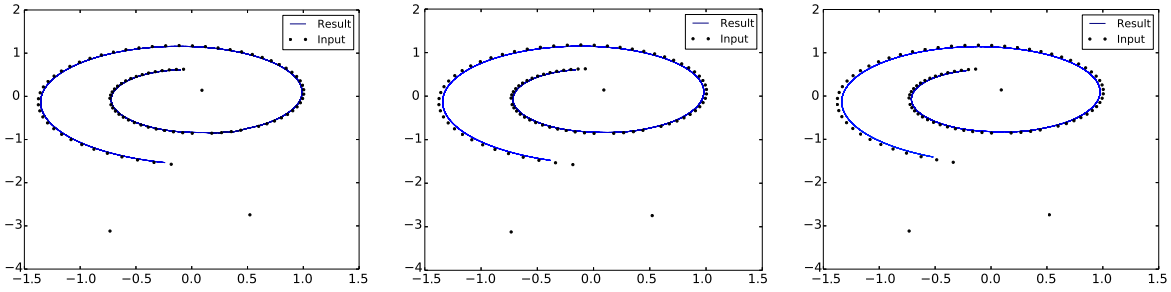

(d) ℓ_1 scheme D_6. (e) ℓ_1 scheme D_7. (f) ℓ_1 scheme D_8.

Fig. 6. Effect of outliers on fitting curves: Three outliers are presented in an initial data. Initial data generated by parametric curve is shown by solid filled circles while fitted curves are shown by solid lines.

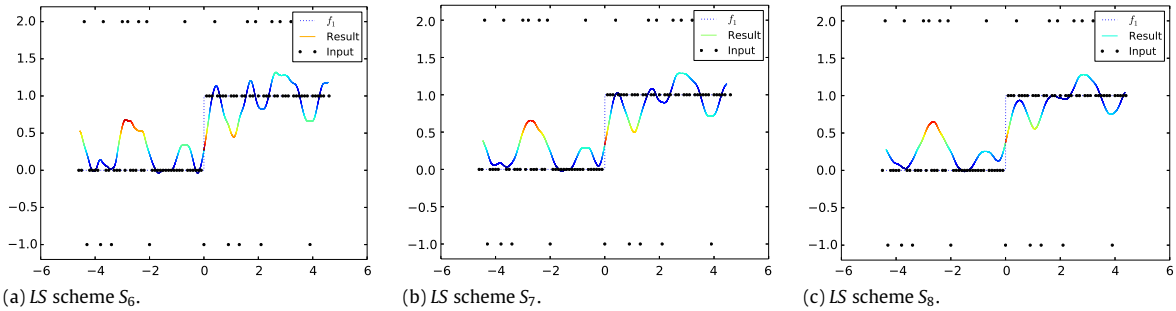

(a) *LS* scheme S_6. (b) *LS* scheme S_7. (c) *LS* scheme S_8.

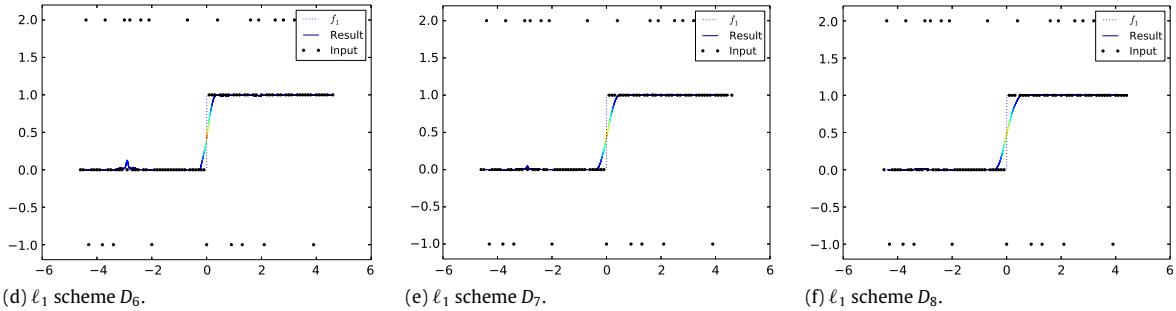

(d) ℓ_1 scheme D_6. (e) ℓ_1 scheme D_7. (f) ℓ_1 scheme D_8.

Fig. 7. Effect of impulsive noises on fitting curves: The input data is corrupted by 25% impulsive noises. Solid curves are generated by *LS*, ℓ_1 schemes.

Experiment 3: In third experiment, we generate data from parametric curve (i.e logarithmic spiral)

$$x(t) = \cos(t)e^{0.1t},$$
$$y(t) = \sin(t)e^{0.1t},$$

along with three outliers. Our findings in Experiment 1 and 2 are also supported by third experiment. Curves fitted by *LS* schemes S_6, S_7 and S_8 are shown in Fig. 6(a)–(c) while fitted curves by ℓ_1 schemes are shown in Fig. 6(d)–(f). From this figure, we observe that curves fitted by ℓ_1 schemes do not notice outliers while curves fitted by *LS* schemes compromise with outliers.

Experiment 4: In this experiment, we consider the data with 25% impulsive noises. In order to restore data corrupted with impulsive noises, we use ℓ_1 and *LS* schemes. Fig. 7 illustrates the fitting curves on restored data by ℓ_1 and *LS* schemes.

3. ℓ_1 scheme for surface fitting

In this section, we generalize our representation of Section 2.2 to the 3-dimensional case. That is, we focus our attention to introduce ℓ_1 scheme for surface based on fitting of a 2-dimensional line function $f(x, y) = \beta_1 + \beta_2 x + \beta_3 y$ to $4n^2$ observations ($x_r = r, y_s = s, f_{r,s}$) for $-n + 1 \leqslant r, s \leqslant n$, for $n \geqslant 1$ in 3-dimensional

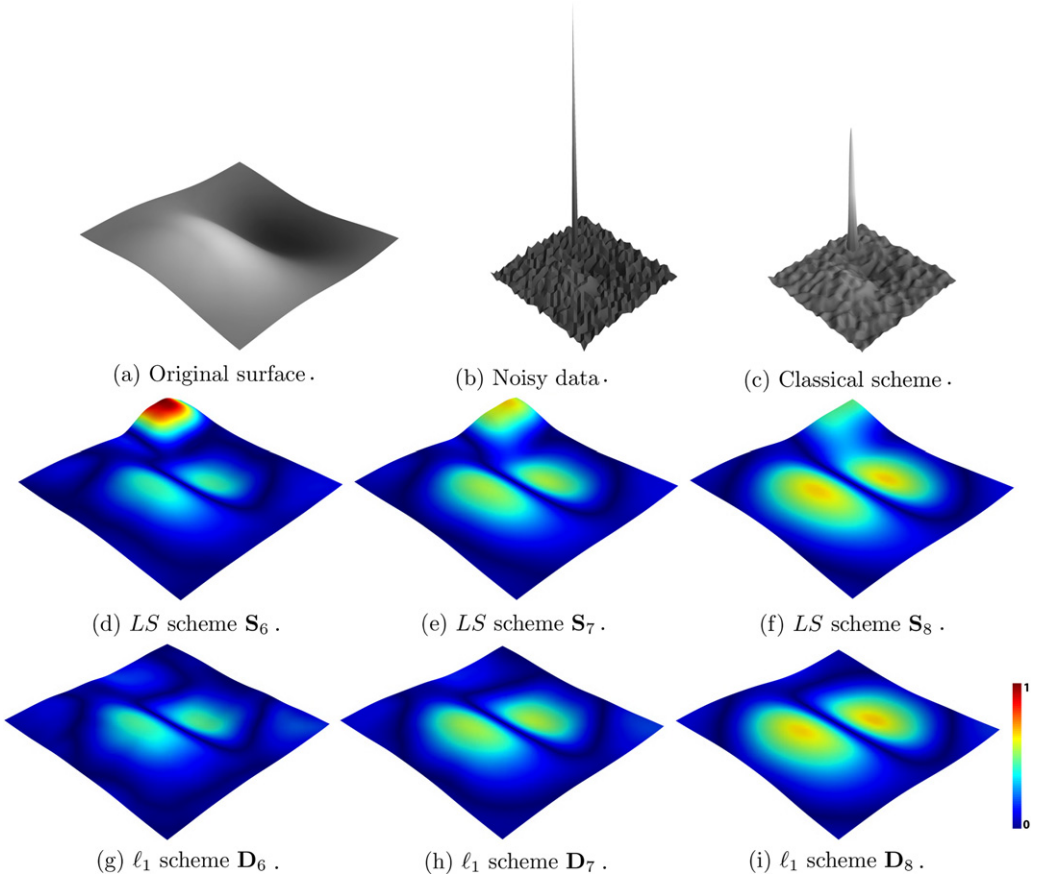

Fig. 8. Functional surface reconstructed from highly noisy functional data with outlier by ℓ_1, LS and classical schemes.

space by IRLS procedure. All that needed, is to take derivative of following iterative formula

$$\beta_{1,\delta}^{(m+1)}, \beta_{2,\delta}^{(m+1)}, \beta_{3,\delta}^{(m+1)} = \arg \min_{\beta_1,\beta_2 \in \mathbb{R}} \sum_{r=-n+1}^{n} \sum_{s=-n+1}^{n} w_{r,s}^{(m)} \left(f_{r,s} - \beta_1 - r\beta_2 - s\beta_3\right)^2,$$

where $w_{r,s}^{(m)} = 1/\left[\left(f_{r,s} - \beta_{1,\delta}^{(m)} - r\beta_{2,\delta}^{(m)} - s\beta_{3,\delta}^{(m)}\right)^2 + \delta\right]^{1/2}$ and setting them to zero. This leads to the system of linear equations. For solving this system we get $\beta_{1,\delta}^{(m+1)}$, $\beta_{2,\delta}^{(m+1)}$ and $\beta_{3,\delta}^{(m+1)}$.

By substituting optimum $\beta_{1,\delta}^{(m+1)}$, $\beta_{2,\delta}^{(m+1)}$, $\beta_{3,\delta}^{(m+1)}$ of β_1, β_2, β_3 into the linear function $f(x, y) = \beta_1 + \beta_2 x + \beta_3 y$ and evaluating this function at (1/4,1/4), (3/4,1/4), (1/4,3/4), (3/4,3/4) then changing notations, we get closed form of ℓ_1 scheme for surface fitting of noisy data with impulsive noises and outliers shown in Appendix B.

3.1. Numerical experiments

This section uses numerical experiments to demonstrate performance and accuracy of our ℓ_1 and LS surface schemes. Same with the curve examples, we use the jet colorbar to display the fitting error for each point on the reconstruction surface. The colorbar is shown in Fig. 8 and the fitting errors are normalized to [0, 1].

Experiment 1: Consider the function

$$z = F(x, y) = xe^{-x^2-y^2}.$$

By taking randomly distributed points with Gaussian noise of mean zero and variance 0.1 along with one outlier with high amplitude we fit surfaces by ℓ_1 and LS schemes. Fitted surfaces by these schemes are shown in Fig. 8(c)–(i), while original surface and noisy data with outlier are presented in Fig. 8(a) and (b) respectively. From this figure it is observed that outlier leave significant effect on fitting surfaces for low complexity LS scheme but its effect go on decreasing with the increase of complexity of the scheme while ℓ_1 schemes are free from the effect of outlier. However, both schemes have ability to produce smooth surface fitting models. The surface reconstructed by classical scheme i.e. bi-quadratic B-spline is shown in Figure (c). From this figure we conclude that classical schemes are not suitable for fitting such type of data. If $f_{i,j}^{(k)} = (f_{x_{i,j}}^{(k)}, f_{y_{i,j}}^{(k)}, f_{z_{i,j}}^{(k)})$ then the fitting performance is characterized by the fitting error.

$$\text{Error} = \frac{\sum_{i,j} \left[f_{z_{i,j}}^{(k)} - F(f_{x_{i,j}}^{(k)}, f_{y_{i,j}}^{(k)})\right]^2}{N},$$

where N is the total number of fitting values. The mean errors of fitting surfaces shown in Fig. 8 are presented in Table 3.

Table 3
Comparison: Error between fitting surfaces shown in figure surface and actual function F.

LS schemes	S_6	S_7	S_8
Errors	0.004313	0.004887	0.007428
ℓ_1 schemes	D_6	D_7	D_8
Errors	0.002307	0.003898	0.006764

Experiment 2: In this experiment, we consider following parametric surface

$$x(u, v) = \cos(v)(3 + u\cos(v/2)),$$
$$y(u, v) = \sin(v)(3 + u\cos(v/2)),$$

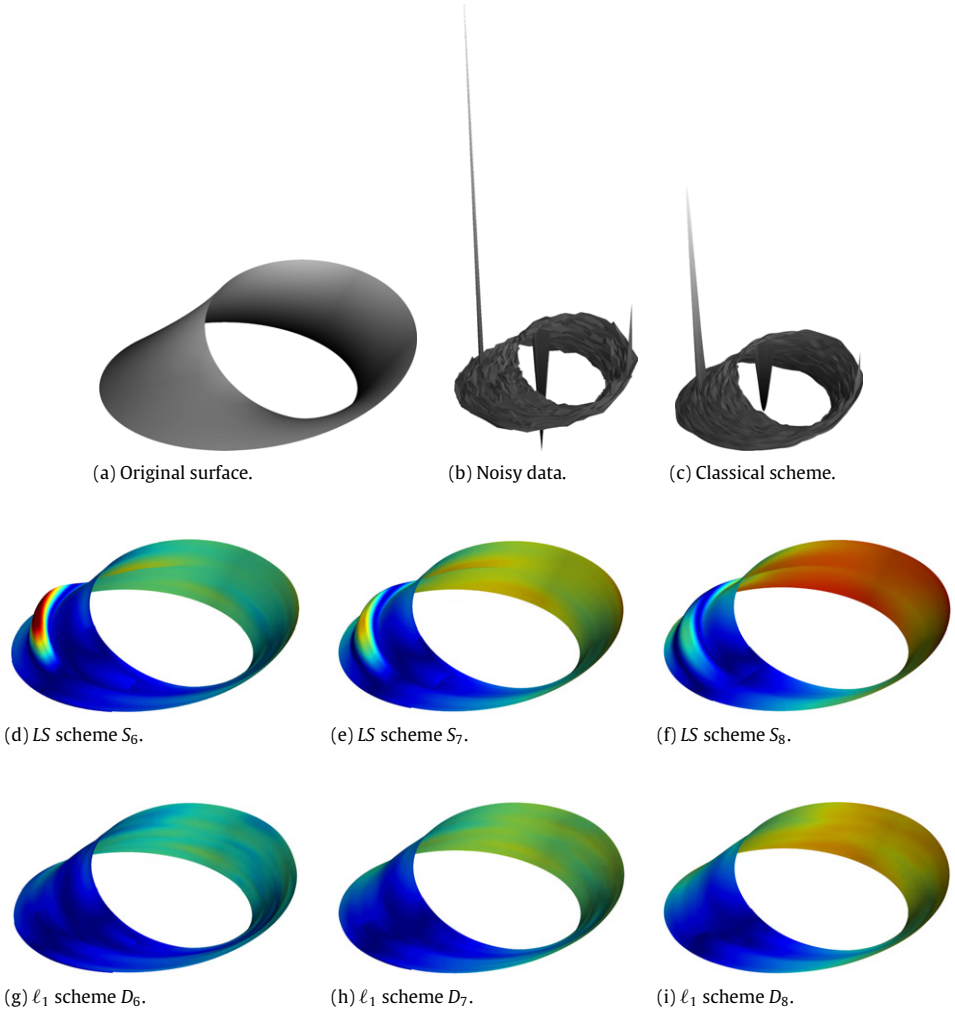

(a) Original surface. (b) Noisy data. (c) Classical scheme.

(d) *LS* scheme S_6. (e) *LS* scheme S_7. (f) *LS* scheme S_8.

(g) ℓ_1 scheme D_6. (h) ℓ_1 scheme D_7. (i) ℓ_1 scheme D_8.

Fig. 9. Parametric surface reconstructed by ℓ_1 and *LS* and classical schemes from highly noisy parametric data with outliers.

$z(u, v) = u \sin(v/2)$.

The data shown in Fig. 9(b) has been generated by taking $-1.5 \leqslant u \leqslant 1.5$, $-1.25 \leqslant v \leqslant 1.25$ (40 values of u and 50 values of v) added with Gaussian noise of mean zero and variance 0.1 along with outliers. Parametric surface has been reconstructed by ℓ_1 and *LS* schemes from data shown in Fig. 9(b). Results have been shown in Fig. 9(c)–(i) while original parametric surface in Fig. 9(a).

4. Conclusion

We have developed ℓ_1-regression based subdivision algorithm with dynamic iterative reweighted weights which has closed form solution for each iteration. It is suitable for curve and surface fitting when the data points are given as exact, or contaminated with random noise, or noisy data with impulsive noises and outliers. Several experiments have been carried out on different types of data such as functional and parametric data along with and without added noise and outliers. These experiments demonstrate that the introduced algorithm can significantly outperform *LS*-regression based subdivision algorithm with constant weights. Compared with *LS*-regression based subdivision algorithm, our algorithm can approximate an input model with a much smaller error. To the best of our knowledge, this is the first subdivision-based algorithm for removal of outliers. The introduction of subdivision-based algorithm for preservation of sharp features in the presence of noise and outliers is the possible future research direction.

Acknowledgments

The authors are grateful for the support provided by 973 Program 2011CB302400, the NSF of China (No. 61303148, No. 11031007 and No. 11371341), NSF of AnHui Province, China (No. 1408085QF119), Ph.D. Programs Foundation of Ministry of Education of China (No. 20133402120002), and the Chinese Academy of Sciences (CAS) fellowship for visiting scholars from developing countries.

Appendix A

A.1. Algorithm for subdivision curve

Let $f_i^{(k)} \in \mathbb{R}^N$, $i \in \mathbb{Z}$, denote a sequence of points in $\mathbb{R}^N$, $N \geqslant 2$, where k is a non negative integer, then ℓ_1 scheme D_{2n} for curve fitting which maps coarse points $f_i^{(k)}$ to refined points $f_i^{(k+1)}$ is defined by (4)

$$f_{2i}^{(k+1)} = \left(\frac{1}{\tau_{1,i}^{(m)}}\right) \sum_{r=-n+1}^{n} \left\{ 1 - \left(\tau_{2,i}^{(m)} - \frac{1}{4}\tau_{1,i}^{(m)}\right) \times \left(\frac{r\tau_{1,i}^{(m)} - \tau_{2,i}^{(m)}}{\tau_{1,i}^{(m)}\tau_{3,i}^{(m)} - \left(\tau_{2,i}^{(m)}\right)^2} \right) \right\} w_{i+r}^{(m)} f_{i+r}^{(k)},$$

$$f_{2i+1}^{(k+1)} = \left(\frac{1}{\tau_{1,i}^{(m)}}\right) \sum_{r=-n+1}^{n} \left\{ 1 - \left(\tau_{2,i}^{(m)} - \frac{3}{4}\tau_{1,i}^{(m)}\right) \times \left(\frac{r\tau_{1,i}^{(m)} - \tau_{2,i}^{(m)}}{\tau_{1,i}^{(m)}\tau_{3,i}^{(m)} - \left(\tau_{2,i}^{(m)}\right)^2} \right) \right\} w_{i+r}^{(m)} f_{i+r}^{(k)} \quad , \tag{4}$$

where

$$\tau_{1,i}^{(m)} = \sum_{r=-n+1}^{n} w_{i+r}^{(m)},$$

$$\tau_{2,i}^{(m)} = \sum_{r=-n+1}^{n} r w_{i+r}^{(m)},$$

$$\tau_{3,i}^{(m)} = \sum_{r=-n+1}^{n} (r)^2 w_{i+r}^{(m)}, \tag{5}$$

for $k \geqslant 0, m \geqslant 0, \delta > 0$,

$$w_{i+r}^{(m)} = \frac{1}{\left[\left(f_{i+r}^{(k)} - \beta_{1,\delta,i}^{(m)} - r\beta_{2,\delta,i}^{(m)}\right)^2 + \delta\right]^{1/2}}, \tag{6}$$

for $m \geqslant 1$,

$$\beta_{2,\delta,i}^{(m)} = \sum_{r=-n+1}^{n} \frac{r\tau_{1,i}^{(m-1)} - \tau_{2,i}^{(m-1)}}{\tau_{1,i}^{(m-1)}\tau_{3,i}^{(m-1)} - \left(\tau_{2,i}^{(m-1)}\right)^2} w_{i+r}^{(m-1)} f_{i+r}^{(k)}, \tag{7}$$

$$\beta_{1,\delta,i}^{(m)} = \frac{1}{\tau_{1,i}^{(m-1)}} \sum_{r=-n+1}^{n} w_{i+r}^{(m-1)} f_{i+r}^{(k)} - \beta_{2,\delta,i}^{(m)} \left(\frac{\tau_{2,i}^{(m-1)}}{\tau_{1,i}^{(m-1)}}\right), \tag{8}$$

and for $m = 0$

$$\beta_{2,\delta,i}^{(0)} = \left(\frac{1}{4n^3 - n}\right) \sum_{r=-n+1}^{n} (6r - 3) f_{i+r}^{(k)},$$

$$\beta_{1,\delta,i}^{(0)} = \left(\frac{1}{2n}\right) \sum_{r=-n+1}^{n} f_{i+r}^{(k)} - \frac{1}{2}\beta_{2,\delta,i}^{(0)}. \tag{9}$$

In the above algorithm, D_{2n} means scheme named D_{2n} takes $2n$ consecutive points form initial polygon to compute new point in order to get a refined polygon. Dotted points in Figs. 3–5 are initial points of the initial polygon. For example: for $n = 3$, scheme S_6 use 6 consecutive points form initial polygon to compute new point to get refined polygon.

At the moment we cannot propose an automatic way of selecting δ. However, numerical experiments show that small value of δ is good choice. Sufficiently large value of m is better choice. However, the choice of $m = 5$ or 6 is sufficient.

A.2. Generalization and variants

Thus far in this brief, and for ease of exposition, we have restricted our attention to introduce ℓ_1 scheme based on fitting of a one-dimensional line to $2n$ observations in two-dimensional space by IRLS procedure. A further generalization to yield ℓ_1 scheme of the IRLS procedure can be made by fitting function of the form $f(x) = \sum_{i=1}^{K} \beta_i f_i(x)$, $K > 0$. It is not necessary for the functions f_K to be linear in x-all that is needed is that f is to be a linear combination of these functions.

As a slight variation on ℓ_1 scheme D_{2n}, we suggest the replacement of 1/4 by $-1/4$ and 3/4 by 1/4 in (4), summation from $r = -n+1 \ldots n$ by $r = -n \ldots n$ in (4)–(8), and Eq. (9) by following

$$\beta_{1,\delta,i}^{(0)} = \left(\frac{1}{2n+1}\right) \sum_{r=-n}^{n} f_{i+r}^{(k)},$$

$$\beta_{2,\delta,i}^{(0)} = \frac{1}{n(n+1)(2n+1)} \sum_{r=-n}^{n} 3r f_{i+r}^{(k)}$$

to get $(2n+1)$-point ℓ_1 scheme D_{2n+1}. If weights $w_{i+r}^{(m)} = 1$, $\forall i,\ r,\ m$, then for $n \geqslant 1$, scheme D_{2n+1} changes into following *LS* scheme S_{2n+1}

$$f_{2i}^{(k+1)} = \left(\frac{1}{2n+1}\right) \sum_{r=-n}^{n} \left(1 - \frac{3r}{4n(n+1)}\right) f_{i+r}^{(k)},$$

$$f_{2i+1}^{(k+1)} = \left(\frac{1}{2n+1}\right) \sum_{r=-n}^{n} \left(1 + \frac{3r}{4n(n+1)}\right) f_{i+r}^{(k)}.$$

It is to be noted that for $n = 1$ and $m \geqslant 0$, scheme (4), coincides with classical Chaikin's scheme [29]. However, for $n \geqslant 2$, it is non-symmetric with dynamic weights.

If weights $w_{i+r}^{(m)} = 1, \forall i,\ r,\ m$ in (4), then for $n \geqslant 1$, it changes into following *LS* scheme S_{2n} for curve fitting.

$$f_{2i}^{(k+1)} = \left(\frac{1}{2n}\right) \sum_{j=-n+1}^{n} \left(1 - \frac{6j-3}{8n^2-2}\right) f_{i+j}^{(k)},$$

$$f_{2i+1}^{(k+1)} = \left(\frac{1}{2n}\right) \sum_{j=-n+1}^{n} \left(1 + \frac{6j-3}{8n^2-2}\right) f_{i+j}^{(k)}.$$

Indeed, in this brief we have introduced two special cases S_{2n} and S_{2n+1} of the least square regression based subdivision schemes with constant weights.

Appendix B

B.1. Algorithm for subdivision surface

Let $f_{i,j}^{(k)} \in \mathbb{R}^N$, $i, j \in \mathbb{Z}$, denote a sequence of points in $\mathbb{R}^N$, $N \geqslant 2$, where k is a non negative integer, then ℓ_1 scheme $\mathbf{D}_{2n}$ for surface fitting which maps coarse points $f_{i,j}^{(k)}$ to refined points $f_{i,j}^{(k+1)}$ is defined by (10), where

$$f_{2i,2j}^{(k+1)} = \sum_{r=-n+1}^{n} \sum_{s=-n+1}^{n} \frac{\psi_{1,i,j}^{(m)}}{\kappa_{i,j}^{(m)}} \times \left(1 + \frac{\psi_{2,i,j}^{(m)}}{4\psi_{1,i,j}^{(m)}} + \frac{\psi_{3,i,j}^{(m)}}{4\psi_{1,i,j}^{(m)}}\right) w_{i+r,j+s}^{(m)} f_{i+r,j+s}^{(k)},$$

$$f_{2i+1,2j}^{(k+1)} = \sum_{r=-n+1}^{n} \sum_{s=-n+1}^{n} \frac{\psi_{1,i,j}^{(m)}}{\kappa_{i,j}^{(m)}} \times \left(1 + \frac{3\psi_{2,i,j}^{(m)}}{4\psi_{1,i,j}^{(m)}} + \frac{\psi_{3,i,j}^{(m)}}{4\psi_{1,i,j}^{(m)}}\right) w_{i+r,j+s}^{(m)} f_{i+r,j+s}^{(k)},$$

$$f_{2i,2j+1}^{(k+1)} = \sum_{r=-n+1}^{n} \sum_{s=-n+1}^{n} \frac{\psi_{1,i,j}^{(m)}}{\kappa_{i,j}^{(m)}} \times \left(1 + \frac{\psi_{2,i,j}^{(m)}}{4\psi_{1,i,j}^{(m)}} + \frac{3\psi_{3,i,j}^{(m)}}{4\psi_{1,i,j}^{(m)}}\right) w_{i+r,j+s}^{(m)} f_{i+r,j+s}^{(k)},$$

$$f_{2i+1,2j+1}^{k+1} = \sum_{r=-n+1}^{n} \sum_{s=-n+1}^{n} \frac{\psi_{1,i,j}^{(m)}}{\kappa_{i,j}^{(m)}} \times \left(1 + \frac{3\psi_{2,i,j}^{(m)}}{4\psi_{1,i,j}^{(m)}} + \frac{3\psi_{3,i,j}^{(m)}}{4\psi_{1,i,j}^{(m)}}\right) w_{i+r,j+s}^{(m)} f_{i+r,j+s}^{(k)}, \tag{10}$$

where

$$\psi_{1,i,j}^{(m)} = \lambda_{1,i,j}^{(m)} - \lambda_{2,i,j}^{(m)} r + \lambda_{3,i,j}^{(m)} s,$$
$$\psi_{2,i,j}^{(m)} = -\lambda_{2,i,j}^{(m)} + \lambda_{4,i,j}^{(m)} r - \lambda_{5,i,j}^{(m)} s,$$
$$\psi_{3,i,j}^{(m)} = \lambda_{3,i,j}^{(m)} - \lambda_{5,i,j}^{(m)} r + \lambda_{6,i,j}^{(m)} s, \tag{11}$$

$$\kappa_{i,j}^{(m)} = \tau_{1,i,j}^{(m)} \tau_{4,i,j}^{(m)} \tau_{6,i,j}^{(m)} - \tau_{1,i,j}^{(m)} \left(\tau_{5,i,j}^{(m)}\right)^2 - \left(\tau_{2,i,j}^{(m)}\right)^2 \tau_{6,i,j}^{(m)} + 2\tau_{2,i,j}^{(m)} \tau_{3,i,j}^{(m)} \tau_{5,i,j}^{(m)} - \left(\tau_{3,i,j}^{(m)}\right)^2 \tau_{4,i,j}^{(m)}, \tag{12}$$

$$\lambda_{1,i,j}^{(m)} = \tau_{4,i,j}^{(m)} \tau_{6,i,j}^{(m)} - \left(\tau_{5,i,j}^{(m)}\right)^2, \lambda_{2,i,j}^{(m)} = \tau_{2,i,j}^{(m)} \tau_{6,i,j}^{(m)} - \tau_{3,i,j}^{(m)} \tau_{5,i,j}^{(m)},$$
$$\lambda_{3,i,j}^{(m)} = \tau_{2,i,j}^{(m)} \tau_{5,i,j}^{(m)} - \tau_{3,i,j}^{(m)} \tau_{4,i,j}^{(m)}, \lambda_{4,i,j}^{(m)} = \tau_{1,i,j}^{(m)} \tau_{6,i,j}^{(m)} - \left(\tau_{3,i,j}^{(m)}\right)^2,$$
$$\lambda_{5,i,j}^{(m)} = \tau_{1,i,j}^{(m)} \tau_{5,i,j}^{(m)} - \tau_{2,i,j}^{(m)} \tau_{3,i,j}^{(m)}, \lambda_{6,i,j}^{(m)} = \tau_{1,i,j}^{(m)} \tau_{4,i,j}^{(m)} - \left(\tau_{2,i,j}^{(m)}\right)^2, \tag{13}$$

$$\tau_{1,i,j}^{(m)} = \sum_{r=-n+1}^{n} \sum_{s=-n+1}^{n} w_{i+r,j+s}^{(m)}, \tau_{2,i,j}^{(m)} = \sum_{r=-n+1}^{n} \sum_{s=-n+1}^{n} r w_{i+r,j+s}^{(m)},$$
$$\tau_{3,i,j}^{(m)} = \sum_{r=-n+1}^{n} \sum_{s=-n+1}^{n} s w_{i+r,j+s}^{(m)}, \tau_{4,i,j}^{(m)} = \sum_{r=-n+1}^{n} \sum_{s=-n+1}^{n} r^2 w_{i+r,j+s}^{(m)},$$
$$\tau_{5,i,j}^{(m)} = \sum_{r=-n+1}^{n} \sum_{s=-n+1}^{n} rs w_{i+r,j+s}^{(m)}, \tau_{6,i,j}^{(m)} = \sum_{r=-n+1}^{n} \sum_{s=-n+1}^{n} s^2 w_{i+r,j+s}^{(m)}, \tag{14}$$

for $k \geqslant 0, m \geqslant 0, \delta > 0$,

$$w_{i+r,j+s}^{(m)} = \frac{1}{\left[\left(f_{i+r,j+s}^{(k)} - \left(\beta_{1,\delta,i,j}^{(m)} + r\beta_{2,\delta,i,j}^{(m)} + s\beta_{3,\delta,i,j}^{(m)}\right)\right)^2 + \delta\right]^{1/2}}, \tag{15}$$

for $m \geqslant 1$ use following

$$\beta_{1,\delta,i,j}^{(m)} = \left(\frac{1}{\kappa_{i,j}^{(m-1)}}\right)\left\{\lambda_{1,i,j}^{(m-1)} \chi_{1,i,j}^{(m-1)} - \lambda_{2,i,j}^{(m-1)} \chi_{2}^{(m-1)} + \lambda_{3,i,j}^{(m-1)} \chi_{3,i,j}^{(m-1)}\right\}, \tag{16}$$

$$\beta_{2,\delta,i,j}^{(m)} = \left(\frac{1}{\kappa_{i,j}^{(m-1)}}\right)\left\{-\lambda_{2,i,j}^{(m-1)} \chi_{1,i,j}^{(m-1)} + \lambda_{4,i,j}^{(m-1)} \chi_{2,i,j}^{(m-1)} - \lambda_{5,i,j}^{(m-1)} \chi_{3,i,j}^{(m-1)}\right\}, \tag{17}$$

$$\beta_{3,\delta,i,j}^{(m)} = \left(\frac{1}{\kappa_{i,j}^{(m-1)}}\right)\left\{\lambda_{3,i,j}^{(m-1)} \chi_{1,i,j}^{(m-1)} - \lambda_{5,i,j}^{(m-1)} \chi_{2,i,j}^{(m-1)} + \lambda_{6,i,j}^{(m-1)} \chi_{3,i,j}^{(m-1)}\right\}, \tag{18}$$

$$\chi_{1,i,j}^{(m-1)} = \sum_{r=-n+1}^{n} \sum_{s=-n+1}^{n} w_{i+r,j+s}^{(m-1)} f_{i+r,j+s}^{(k)},$$
$$\chi_{2,i,j}^{(m-1)} = \sum_{r=-n+1}^{n} \sum_{s=-n+1}^{n} r w_{i+r,j+s}^{(m-1)} f_{i+r,j+s}^{(k)},$$
$$\chi_{3,i,j}^{(m-1)} = \sum_{r=-n+1}^{n} \sum_{s=-n+1}^{n} s w_{i+r,j+s}^{(m-1)} f_{i+r,j+s}^{(k)}, \tag{19}$$

and use following for $m = 0, \xi_n = \frac{1}{2n^2(4n^2-1)}$

$$\beta_{1,\delta,i,j}^{(0)} = \frac{1}{2}\xi_n \sum_{r=-n+1}^{n} \sum_{s=-n+1}^{n} (4n^2 + 5 - 6r - 6s) f_{i+r,j+s}^{(k)},$$
$$\beta_{2,\delta,i,j}^{(0)} = 3\xi_n \sum_{r=-n+1}^{n} \sum_{s=-n+1}^{n} (2r-1) f_{i+r,j+s}^{(k)},$$
$$\beta_{3,\delta,i,j}^{(0)} = 3\xi_n \sum_{r=-n+1}^{n} \sum_{s=-n+1}^{n} (2s-1) f_{i+r,j+s}^{(k)}. \tag{20}$$

B.2. Generalizations and variants

We can continue generalization by considering the fitting of a p-dimensional hyperplane to a set of point observations in $(p+1)$-dimensional space. Again using the IRLS as optimality criterion, we obtain ℓ_1 scheme for the fitting of the hyperplane to this set of observations. A further slight generalization of ℓ_1 scheme (10) can be made based on fitting of a 2-dimensional polynomial of degree $\geqslant 2$ to $4n^2$ observations $(x_r = r, y_s = s, f_{r,s})$ for $-n+1 \leqslant r, s \leqslant n$, for $n \geqslant 1$ in 3-dimensional space by IRLS procedure.

Here we present some variants of ℓ_1 scheme. If weights $w_{i+r,j+s}^{(m)} = 1, \forall i, j, r, s, m$ in (10) then for $n \geqslant 1$, we get following new *LS* scheme $\mathbf{S}_{2n}$ to handle noisy data.

$$f_{2i,2j}^{(k+1)} = \frac{1}{4}\xi_n \sum_{r=-n+1}^{n} \sum_{s=-n+1}^{n} \left(8n^2 - 6r - 6s + 4\right) f_{r,s}^{(k)},$$
$$f_{2i+1,2j}^{(k+1)} = \frac{1}{4}\xi_n \sum_{r=-n+1}^{n} \sum_{s=-n+1}^{n} \left(8n^2 + 6r - 6s - 2\right) f_{r,s}^{(k)},$$
$$f_{2i,2j+1}^{(k+1)} = \frac{1}{4}\xi_n \sum_{r=-n+1}^{n} \sum_{s=-n+1}^{n} \left(8n^2 - 6r + 6s - 2\right) f_{r,s}^{(k)},$$
$$f_{2i+1,2j+1}^{(k+1)} = \frac{1}{4}\xi_n \sum_{r=-n+1}^{n} \sum_{s=-n+1}^{n} \left(8n^2 + 6r + 6s - 8\right) f_{r,s}^{(k)}.$$

Here is the another slight variant of ℓ_1 scheme $\mathbf{D}_{2n}$ (10).

Lemma 1. *Let $f_{i,j}^{(k)} \in \mathbb{R}^N, i, j \in \mathbb{Z}$, denote a sequence of points in $\mathbb{R}^N, N \geqslant 2$, where k is a non negative integer, then ℓ_1 scheme $\mathbf{D}_{2n+1}$ for surface fitting which maps coarse points $f_{i,j}^{(k)}$ to refined points $f_{i,j}^{(k+1)}$ is defined by (10) with some variants i.e. replace $1/4$ by $-1/4$, $3/4$ by $1/4$ in (10) and take summation from $-n, \ldots, n$ in (10)–(19), and for $m = 0$ use following instead of (20)*

$$\beta_{1,\delta,i,j}^{(0)} = \frac{1}{(2n+1)^2} \sum_{r=-n}^{n} \sum_{s=-n}^{n} f_{i+r,j+s}^{(k)},$$
$$\beta_{2,\delta,i,j}^{(0)} = \frac{3}{n(n+1)(2n+1)^2} \sum_{r=-n}^{n} \sum_{s=-n}^{n} r f_{i+r,j+s}^{(k)},$$
$$\beta_{3,\delta,i,j}^{(0)} = \frac{3}{n(n+1)(2n+1)^2} \sum_{r=-n}^{n} \sum_{s=-n}^{n} s f_{i+r,j+s}^{(k)}.$$

If weights $w_{i+r,j+s}^{(m)} = 1, \forall i, j, r, s, m$ in ℓ_1 scheme $\mathbf{D}_{2n+1}$ then for $n \geqslant 1$, we get following new *LS* scheme $\mathbf{S}_{2n+1}$ for surface fitting.

$$f_{2i,2j}^{(k+1)} = \frac{1}{(2n+1)^2} \sum_{r=-n}^{n} \sum_{s=-n}^{n} \left(1 + \frac{-3r - 3s}{4n(n+1)}\right) f_{r,s}^{(k)},$$
$$f_{2i+1,2j}^{(k+1)} = \frac{1}{(2n+1)^2} \sum_{r=-n}^{n} \sum_{s=-n}^{n} \left(1 + \frac{3r - 3s}{4n(n+1)}\right) f_{r,s}^{(k)},$$
$$f_{2i,2j+1}^{(k+1)} = \frac{1}{(2n+1)^2} \sum_{r=-n}^{n} \sum_{s=-n}^{n} \left(1 + \frac{-3r + 3s}{4n(n+1)}\right) f_{r,s}^{(k)},$$
$$f_{2i+1,2j+1}^{(k+1)} = \frac{1}{(2n+1)^2} \sum_{r=-n}^{n} \sum_{s=-n}^{n} \left(1 + \frac{3r + 3s}{4n(n+1)}\right) f_{r,s}^{(k)}.$$

The iterative illustration of ℓ_1 schemes $\mathbf{D}_{2n}$, $\mathbf{D}_{2n+1}$ is similar to the discussion presented in Section 2.3.

References

[1] Sheather SJ. A moden approach to regression with residual, Springer Science, Business Media, LLC 2009.

[2] Sohn B-Y, Kim G-B. Detection of outliers in weighted least squares regression. Korean J Comput Appl Math 1997;4(2):441–52.

[3] Khan MHA, Aktar S. Multiple-case outlier detection in least-squares regression model using quantum-inspired evolutionary algorithm, in Proceeding of 12th international conference on computers and information technology (ICCIT 2009). Dhaka Bangladesh. 2009.

[4] Chartrand R, Yin W. Iteratively reweighted algorithms for compressive sensing. in proceeding of international conference on acoustics, speech, and signal processing (ICASSP'08). pp. 3869–3872, 2008.

[5] Daubechies I, Devore R, Fornasier M, Güntük CS. Iteratively reweigted least squares minimization for sparse recovery. Commun Pure Appl Math 2010;63: 1–38.

[6] Mohan K, Fazel M. Iterative reweigted least squares for matrix rank minimization, in 48th annual allerton conference on communication, control, and computing. pp. 653–661, 2010.

[7] Bissantz N, Dumbgen L, Munk A, Stratmann B. Convergence analysis of generalized iteratively reweighted least squares algorithms on convex function spaces. SIAM J Optim 2009;19:1828–45.

[8] Lai M-J, Xu Y-Y, Yin W-T. Improved iteratively reweighted least squares for unconstrained smoothed l_q minimization. SIAM J Numer Anal 2013;51(2): 927–57.

[9] Pan T, Huang B, Khare S. A practical algorithm to outlier detection and data cleaning for the time-dependant signal. Proceeding of the 32nd chinese control conference. 2013.

[10] Nikolova M. A variational approach to remove outliers and impulse noise. J Math Imaging Vis 2004;20:99–120.

[11] Avron H, Sharf A, Greif C, Cohen-Or D. ℓ_1-Sparse reconstruction of sharp point set surfaces. J ACM Trans Graph 2010;29(5): Article No. 135.

[12] Parsopoulos KE, Kontogianni VA, Pytharouli SI, Psimoulis PA, Stiros SC, Vrahatis MN. Greece, Optimal fitting of curves in monitoring data using the ℓ_1, ℓ_2 and ℓ_∞ norms, INGEO 2004 and FIG regional central and eastern european conference on engineering surveying bratislava, Slovakia, November 11–13. 2004.

[13] Candes E, Romberg J, Tao T. Robust uncertainty principles: exact signal reconstruction from highly incomplete frequency information. IEEE Trans Inform Theory 2006;52(2):489–509.

[14] Goldstein T, Osher S. The split bregman method for L1-regularized problems. SIAM J Imaging Sci 2009;2(2):323–43.

[15] Yang J, Zhang Y. Alternating direction algorithm for ℓ_1-problems in compressing sensing. SIAM J Sci Comput 2011;33(1):250–78.

[16] Liu X, Huang L. A new nonlocal total variation regularization algorithm for image denoising. Math Comput Simulation 2014;97:224–33.

[17] Xiao Y, Zhu H, Wu S-Y. Primal and dual alternating direction algorithms for ℓ_1-, ℓ_1-norm minimization problems in compressive sensing. Comput Optim Appl 2013;54(2):441–59.

[18] Candès EJ, Wakin MB, Boyd SP. Enhancing sparsity by reweighted ℓ_1 minimization. J Fourier Anal Appl 2008;14:877–905.

[19] Dodgson NA, Floater MS, Sabin M. Advances in multiresolution for geometric modeling. Berlin, Heidelberg: Springer-Verlag; 2005.

[20] Dyn N. In: Light W, editor. Sbdivision schemes in computer-aided geometric design. Advances in numerical analysis, vol. II. New York: Oxford University Press; 1992. p. 36–104.

[21] Dyn N, Levin D. Subdivision schemes in geometric modelling. Acta Numer 2002;11:73–144.

[22] Peters J, Reif U. Subdivision surfaces, vol. 3. Springer; 2008.

[23] Sabin M. Analysis and deisgn of univariate subdivision schemes. Berlin, Heidelberg: Springer-Verlag; 2010.

[24] Ivekovic S, Trucco E. Fitting subdivision surface models to noisy and incomplete 3-D data. Lecture notes in computer science, vol. 4418. Springer; 2007. p. 542–54.

[25] Dyn N, Head A, Hormann K, Sharon N. Univariate subdivision schemes for noisy data. CoRR. abs/1307.2990. 2014.

[26] Farebrother RW. L_1-norm and L_∞-norm estimation: an introduction to the least absolute residuals, the minimax absolute residual and related fitting procedures. Springer series in statistics, Heidelberg, New York: Springer; 2013.

[27] Rey W. Introduction to robust and quasi-robust statistical methods. New York: Springer-Verlag; 1983.

[28] Vogel CR, Oman ME. Iterative methods for total variation denoising. SIAM J Sci Comput 1996;17:227–38.

[29] Chaikin GM. An algorithm for high speed curve genration. Comput Graph Image Process 1974;3(4):346–9.